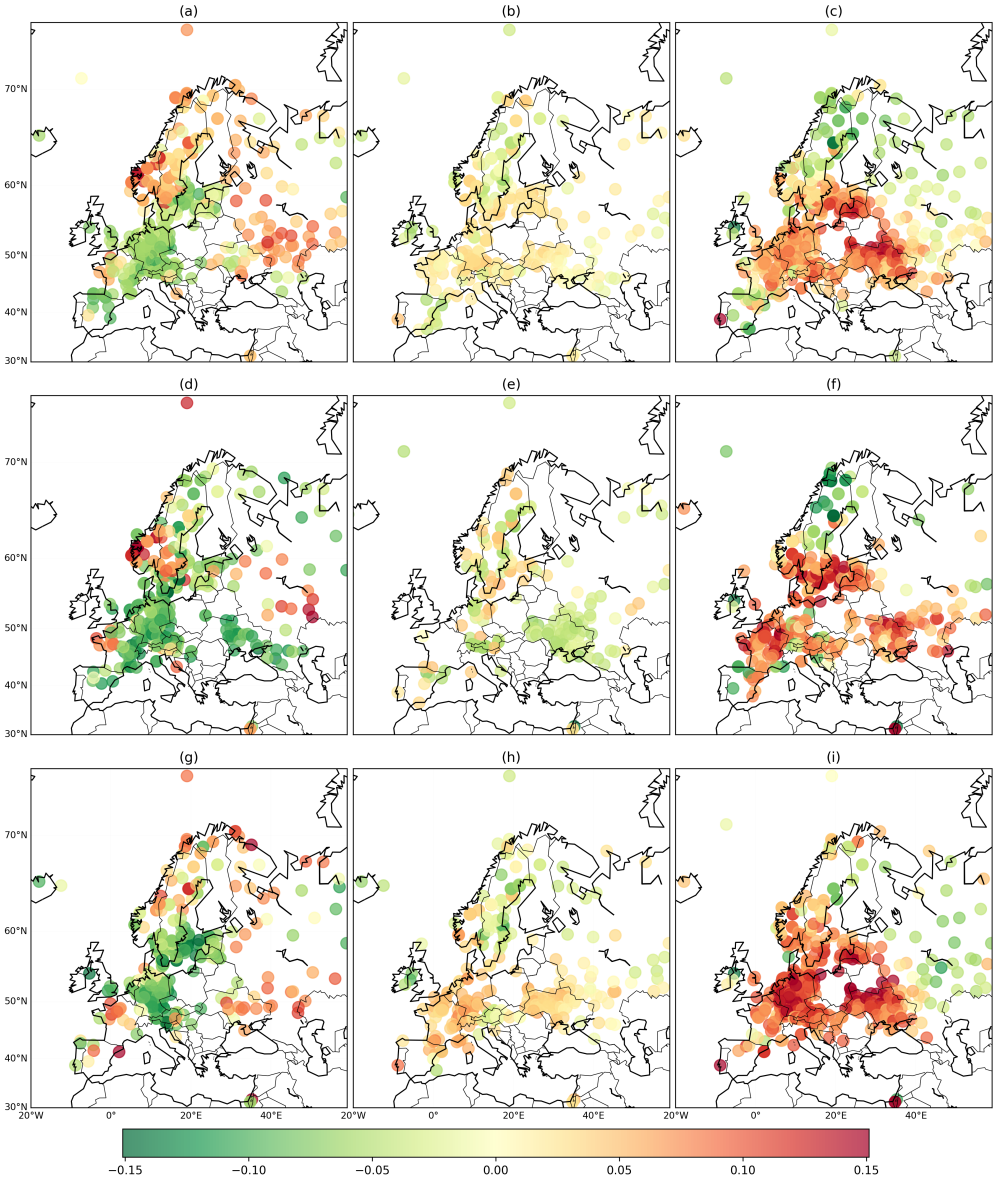
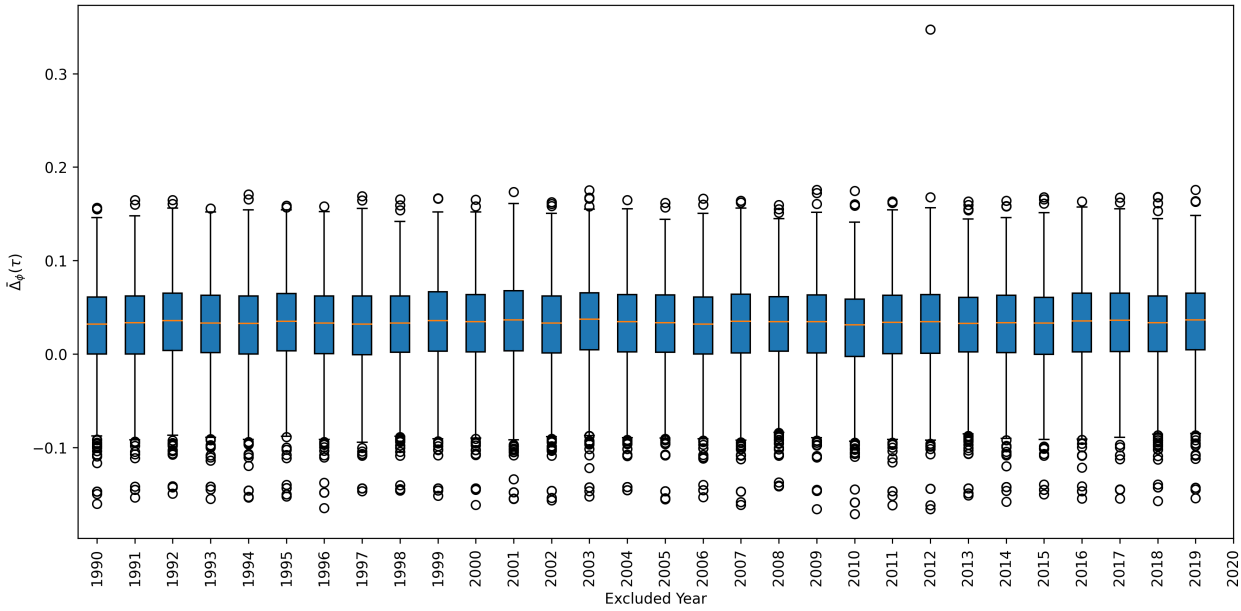
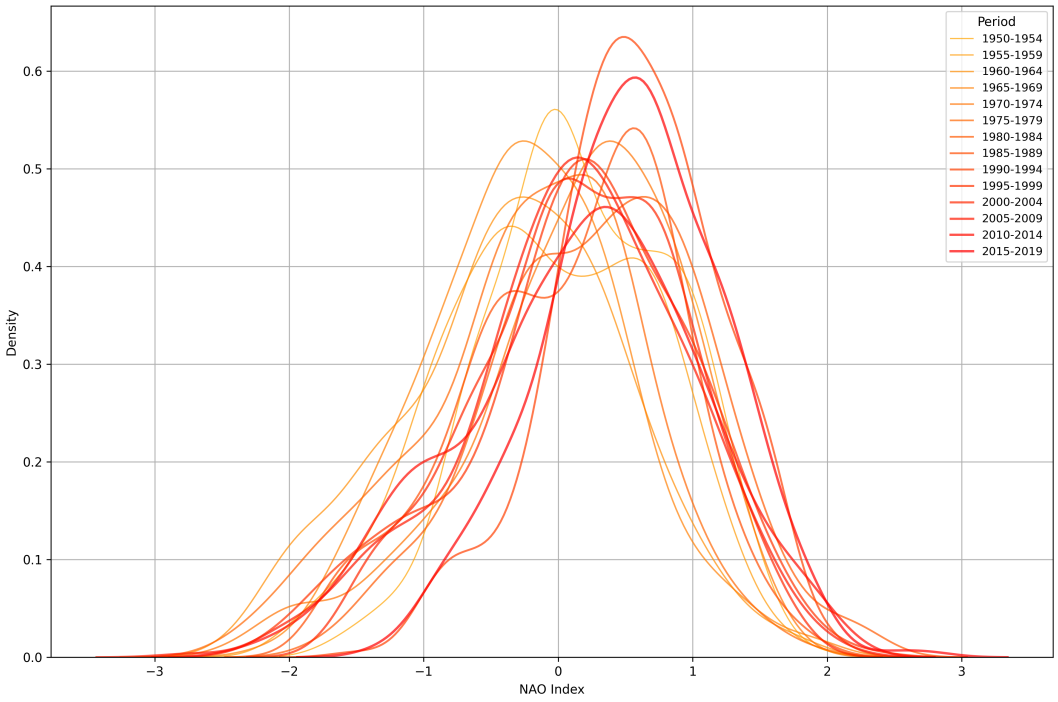
Supplementary Information



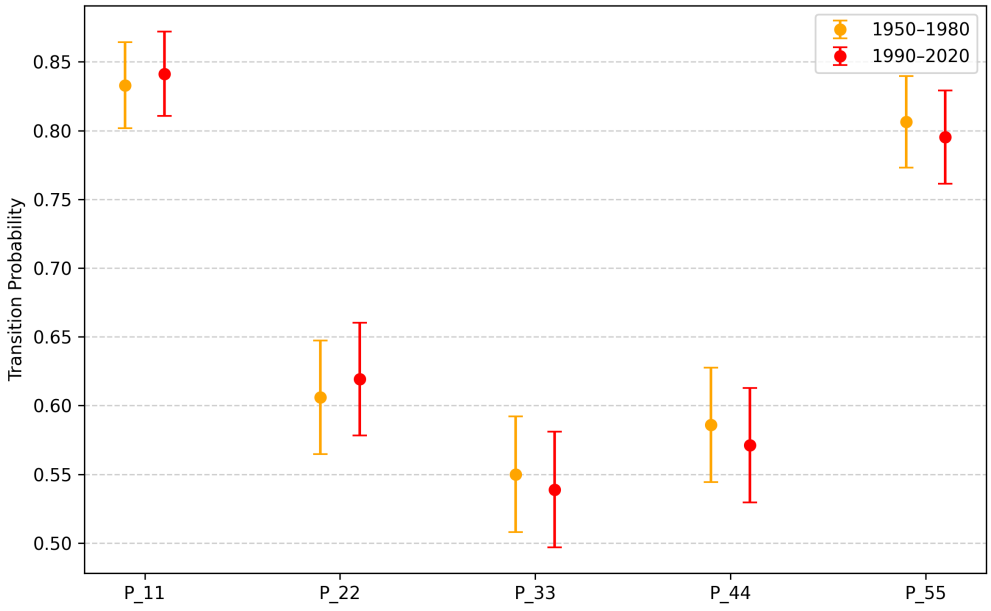
Supplementary Figure 1: Figure 3 where we filtered out the insignificant $\bar{\Delta}_{\phi_t}$ and $\bar{\Delta}_{\psi_{t,\cdot}}$ values. (a)-(c): $\bar{\Delta}_{i,\phi}(\tau)$ for weather stations across Europe with (a) $\tau = 0.05$ (b) $\tau = 0.5$ (c) $\tau = 0.95$. (d)-(i): $\bar{\Delta}_{i,\psi_s}(\tau)$ for weather stations across Europe with (d) $\tau = 0.05$ and $s = \text{NAO}-$ (e) $\tau = 0.5$ and $s = \text{NAO}-$, (f) $\tau = 0.95$ and $s = \text{NAO}-$, (g) $\tau = 0.05$ and $s = \text{NAO}+$ (h) $\tau = 0.5$ and $s = \text{NAO}+$, (i) $\tau = 0.95$ and $s = \text{NAO}+$. The blank regions in Poland and Belarus result from the unavailability of data in the ECA dataset (see Data section).



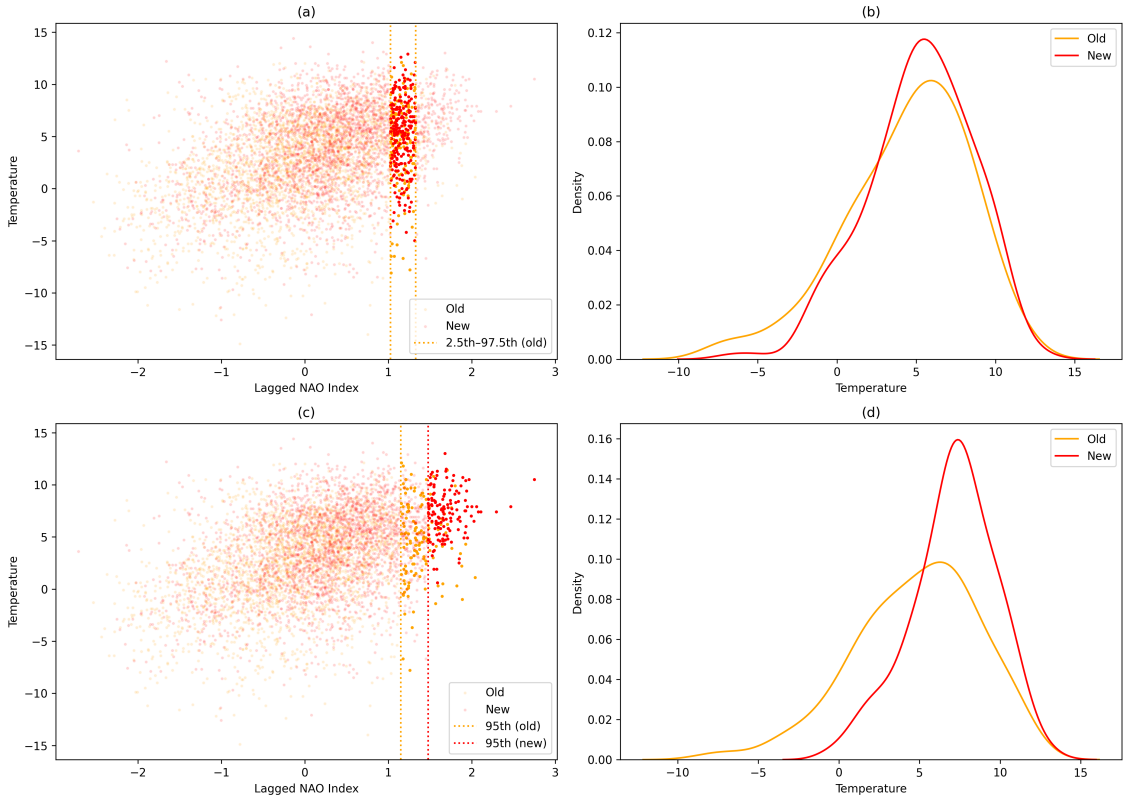
Supplementary Figure 2: Boxplots for $\bar{\Delta}_\phi(\tau)$ for weather stations across Europe when one year is left out using the "new" data. The horizontal axis denotes the year that is excluded from the analysis. The boxplots present the distribution of $\bar{\Delta}_\phi(\tau)$ when one year is excluded.



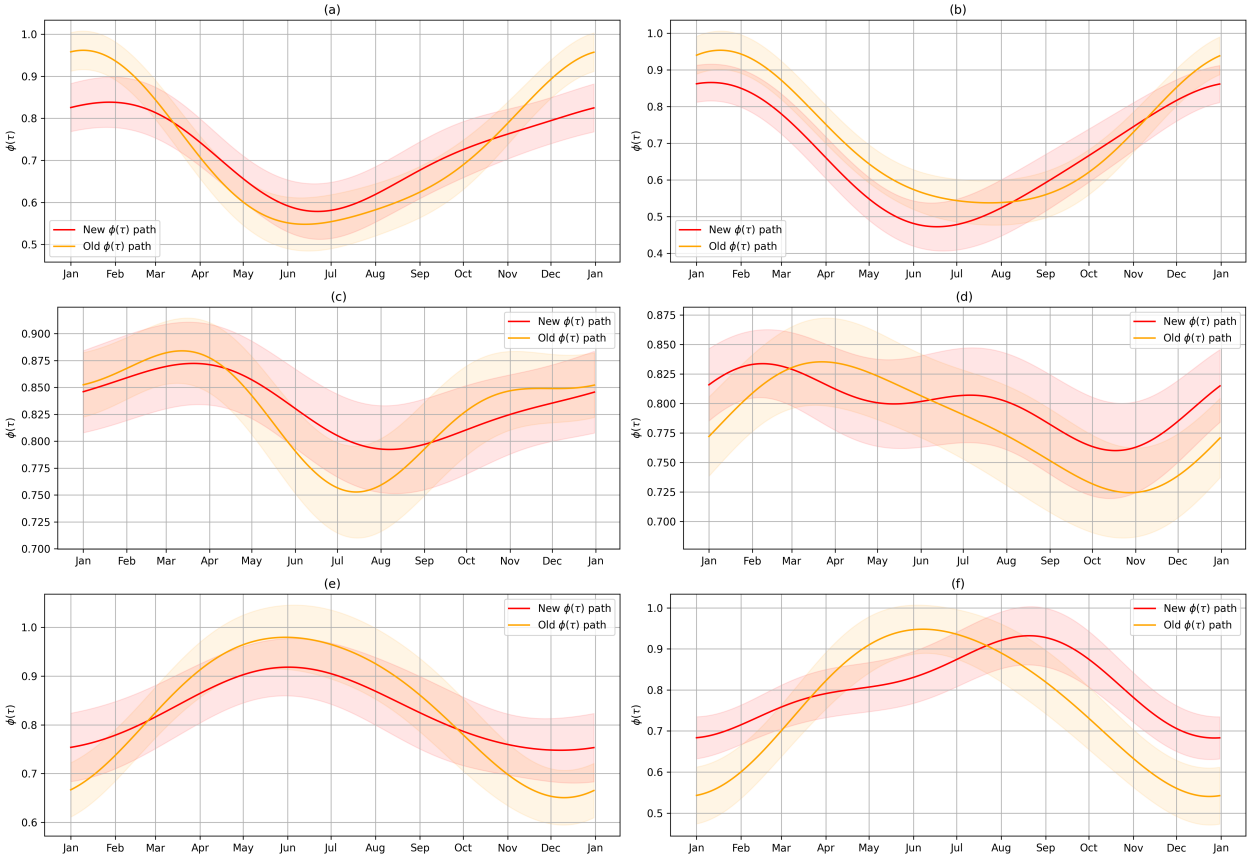
Supplementary Figure 3: NAO index kernel density estimates over time per five years. Lighter (orange) colors indicate older years, whereas darker red colors represent more recent years.



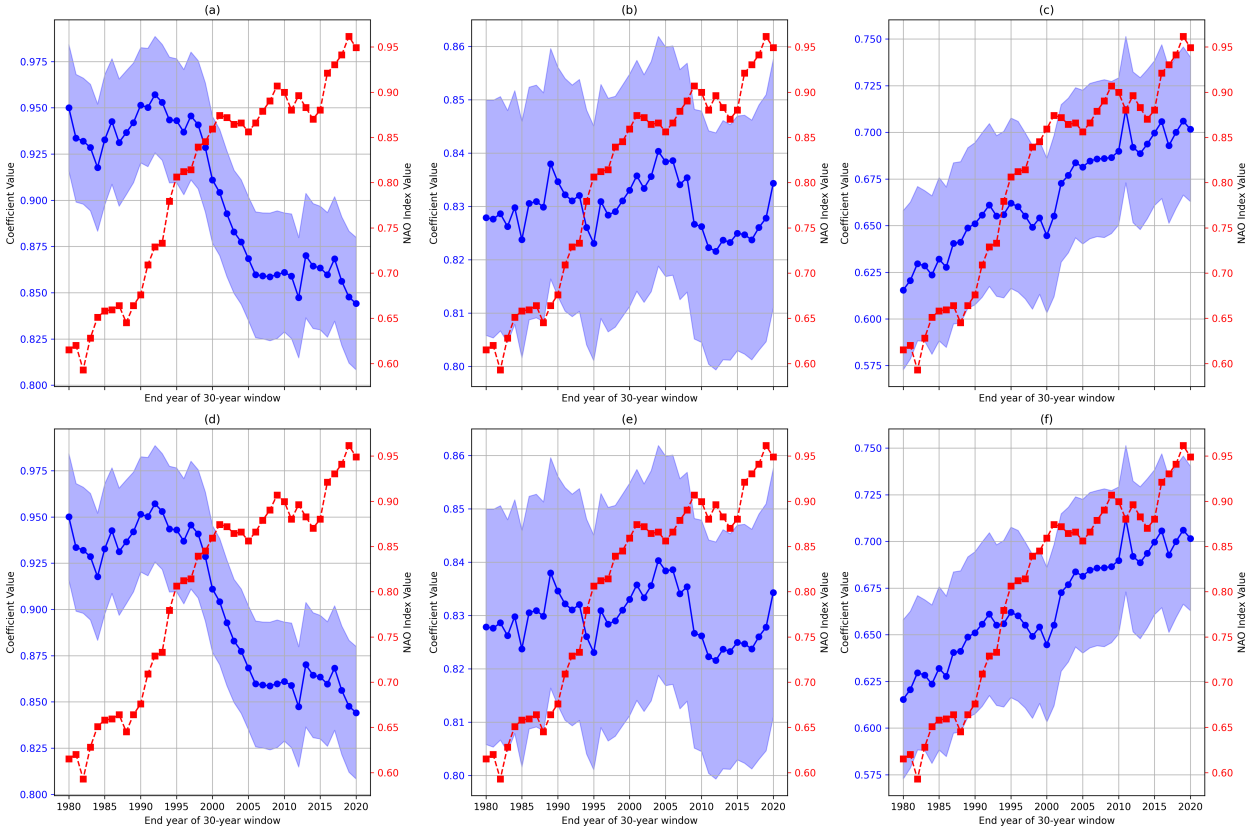
Supplementary Figure 4: Transition probabilities with 95% confidence bounds of the winter NAO index for the quintiles of the "old" (orange) and the "new" (red) data separately. The confidence bounds are obtained by assuming a multinomial distribution for the transition probabilities. A transition probability P_{ij} implies the probability of switching from quintile i to quintile j. For $i = j$ the system stays in the same quintile.



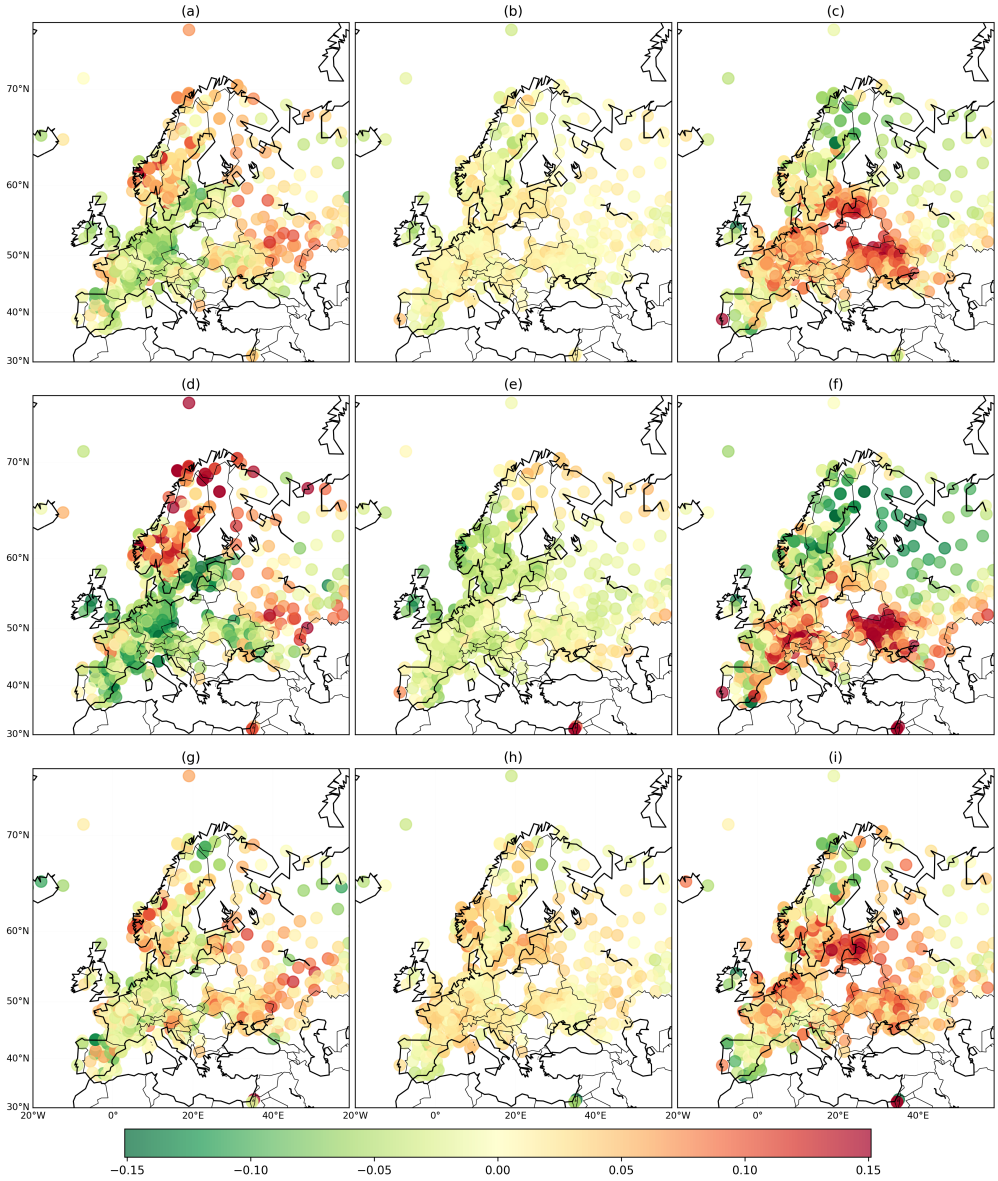
Supplementary Figure 5: All data is in winter (DJF) and for De Bilt. (a) "New" and "old" temperatures vs. lagged NAO index, with dashed lines for the 92.5th and 97.5th percentiles of the "old" NAO index. (b) Kernel density estimate (kde) of temperatures, conditional on the 92.5th–97.5th percentile of the "old" lagged NAO index. (c) "New" and "old" temperatures vs. lagged NAO index, with dashed lines for the 95th percentile of "old" and "new" NAO index. (d) kde of temperatures, conditional on the highest 95% of lagged NAO index values.



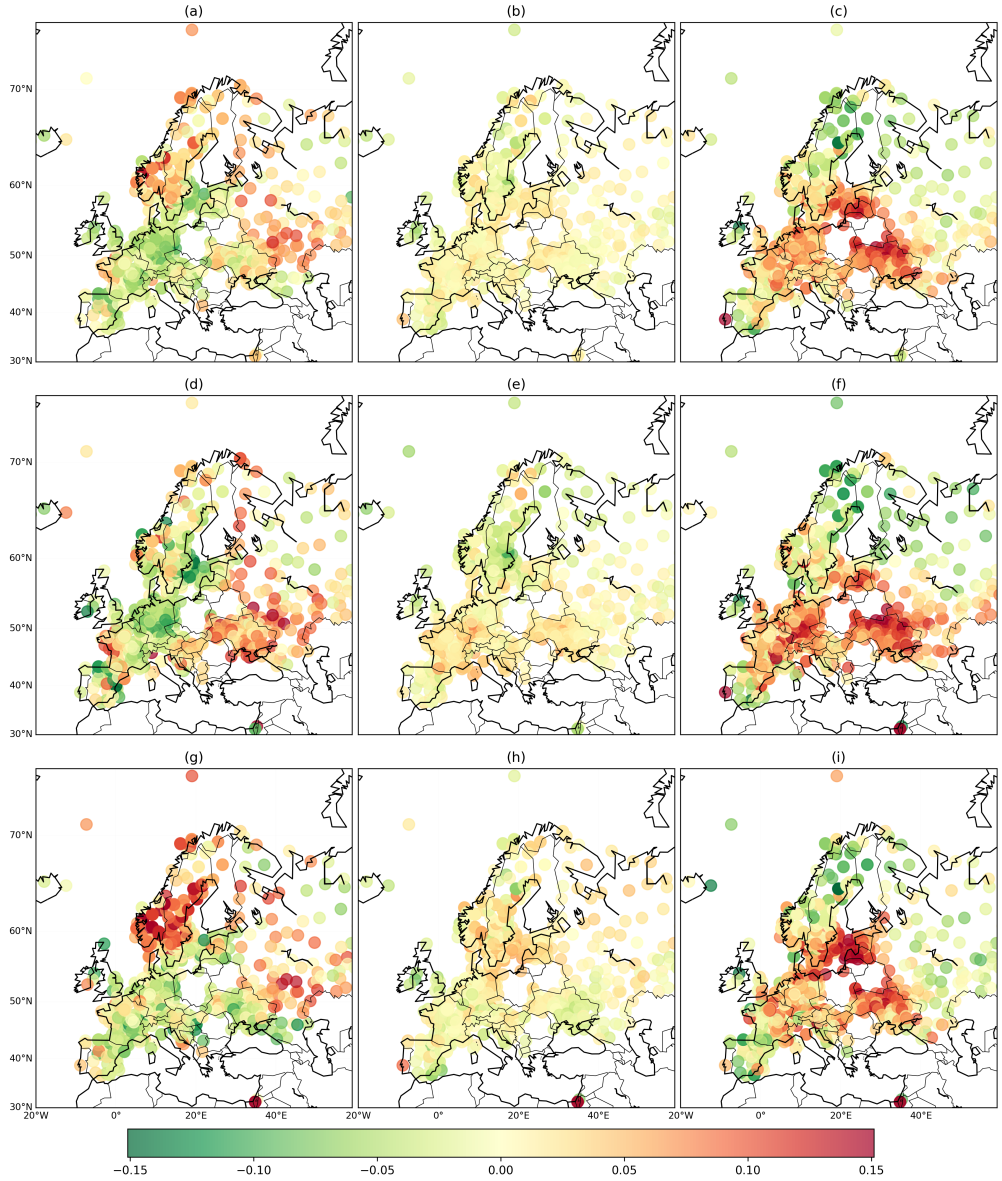
Supplementary Figure 6: Persistence coefficients plots obtained by fitting Model (2) to data for De Bilt. Shaded areas represent 95% pointwise confidence bounds. **(a)** Curves for $\phi_t(\tau)$ fitted on "old" (in orange) and "new" (in red) data with $\tau = 0.05$ conditioned on NAO−. **(b)** Same as (a) but conditioned on NAO+. **(c)** Same as (a) but with $\tau = 0.5$. **(d)** Same as (c) but conditioned on NAO+. **(e)** Same as (a) but with $\tau = 0.95$. **(f)** Same as (e) but conditioned on NAO+.



Supplementary Figure 7: Persistence coefficients $\phi_t(\tau)$ for various values of τ with 95% confidence bounds (in blue) for January 1st based on a 30-year rolling window analysis with ending years 1980–2020 for De Bilt. 80^{th} percentile of the NAO index over time in red. **(a)** $\tau = 0.05$ and $s =$ NAO-. **(b)** $\tau = 0.5$ and $s =$ NAO-. **(c)** $\tau = 0.95$ and $s =$ NAO-. **(d)** $\tau = 0.05$ and $s =$ NAO+. **(e)** $\tau = 0.5$ and $s =$ NAO+. **(f)** $\tau = 0.95$ and $s =$ NAO+.



Supplementary Figure 8: Figure 3 for SCAND. (a)-(c): $\bar{\Delta}_{i,\phi}(\tau)$ for weather stations across Europe with (a) $\tau = 0.05$ (b) $\tau = 0.5$ (c) $\tau = 0.95$. (d)-(i): $\bar{\Delta}_{i,\psi_s}(\tau)$ for weather stations across Europe with (d) $\tau = 0.05$ and $s = \text{SCAND}-$ (e) $\tau = 0.5$ and $s = \text{SCAND}-$, (f) $\tau = 0.95$ and $s = \text{SCAND}-$, (g) $\tau = 0.05$ and $s = \text{SCAND}+$ (h) $\tau = 0.5$ and $s = \text{SCAND}+$, (i) $\tau = 0.95$ and $s = \text{SCAND}+$. The blank regions in Poland and Belarus result from the unavailability of data in the ECA dataset (see Data section).



Supplementary Figure 9: Figure 3 for the AMO. (a)-(c): $\bar{\Delta}_{i,\phi}(\tau)$ for weather stations across Europe with (a) $\tau = 0.05$ (b) $\tau = 0.5$ (c) $\tau = 0.95$. (d)-(i): $\bar{\Delta}_{i,\psi_s}(\tau)$ for weather stations across Europe with (d) $\tau = 0.05$ and $s = \text{AMO}-$ (e) $\tau = 0.5$ and $s = \text{AMO}-$, (f) $\tau = 0.95$ and $s = \text{AMO}-$, (g) $\tau = 0.05$ and $s = \text{AMO}+$ (h) $\tau = 0.5$ and $s = \text{AMO}+$, (i) $\tau = 0.95$ and $s = \text{AMO}+$. The blank regions in Poland and Belarus result from the unavailability of data in the ECA dataset (see Data section).

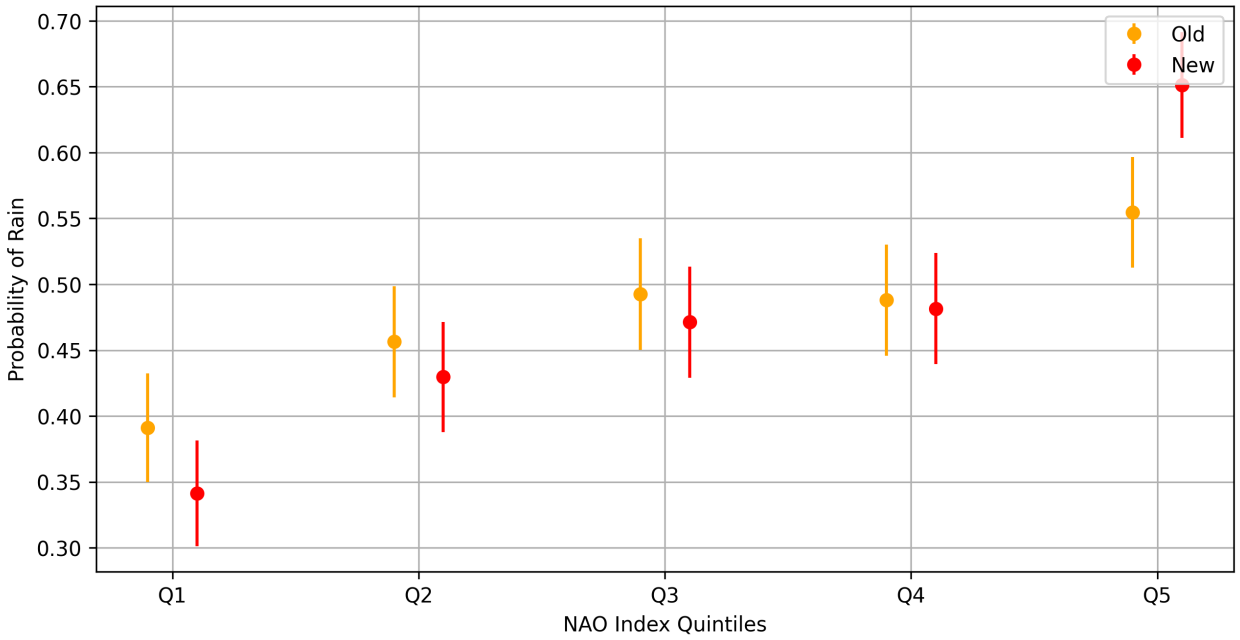
NAO Index Bin	AtR	AtTr	NAO+	NAO−	Neutral	ScBl	ScTr
0–5%	10.6	2.4	0.0	62.0	0.0	24.6	0.3
5–10%	16.2	2.7	0.3	58.2	2.7	19.5	0.3
10–15%	22.2	3.0	0.3	43.5	5.2	25.2	0.6
15–20%	23.6	6.9	2.1	35.0	8.5	22.1	1.8
20–25%	22.1	9.8	3.1	32.2	10.1	21.2	1.5
25–30%	20.4	8.8	5.2	26.8	14.0	21.6	3.0
30–35%	22.1	13.9	3.3	20.6	18.5	18.8	2.7
35–40%	25.4	14.4	4.9	14.1	20.8	17.1	3.4
40–45%	19.5	16.4	6.7	11.2	21.9	18.5	5.8
45–50%	18.6	15.5	8.2	7.6	22.6	18.6	8.8
50–55%	18.9	15.6	5.4	4.2	23.4	19.8	12.6
55–60%	16.4	20.1	12.7	3.4	20.7	15.7	11.1
60–65%	13.4	18.6	14.6	1.5	24.7	14.6	12.5
65–70%	14.3	17.3	17.0	2.4	21.9	11.2	15.8
70–75%	11.6	19.2	14.3	0.6	19.2	10.4	24.7
75–80%	10.6	20.4	20.1	0.9	16.4	8.8	22.8
80–85%	7.6	17.8	25.1	0.0	11.5	8.5	29.6
85–90%	4.3	21.8	23.9	0.3	10.7	7.4	31.6
90–95%	4.3	17.9	31.0	0.0	7.6	4.6	34.7
95–100%	2.1	14.3	31.1	0.0	4.3	0.3	47.9

Supplementary Table 1: Weather regimes on the horizontal axis and 5% NAO index bins on the vertical axis for winter days from 1950-2020. The cells represent the probability of a weather regime as defined by[22], given that the daily NAO index is in a particular 5% bin, where 0–5% and 95–100% represent the lowest and highest 5% of the NAO index in winter, respectively. AtR, AtTr, NAO+, NAO−, ScBl and ScTr denote the Atlantic Ridge, Atlantic Trough, NAO+, NAO−, Scandinavian Blocking and Scandinavian Trough regimes, respectively. Remaining days are classified as Neutral.

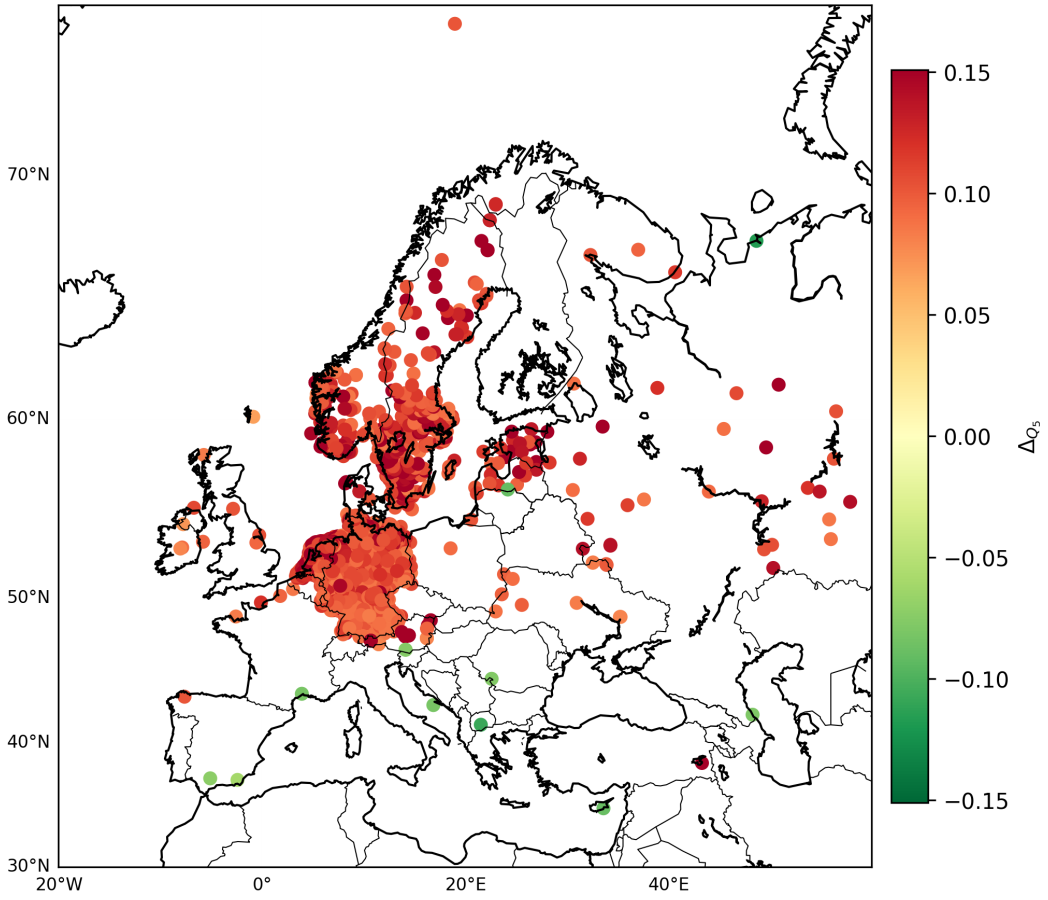
Table 2 shows the "old" and "new" quintiles of the NAO index in winter.

State	1	2	3	4	5
τ	[0, 0.2]	(0.2, 0.4]	(0.4, 0.6]	(0.6, 0.8]	(0.8, 1]
"old"	[-2.5320, -0.7440]	(-0.7440, -0.2584]	(-0.2584, 0.1640]	(0.1640, 0.6152]	(0.6152, 2.0420]
"new"	[-2.7108, -0.3408]	(-0.3408, 0.1488]	(0.1488, 0.5214]	(0.5214, 0.9492]	(0.9492, 2.7513]

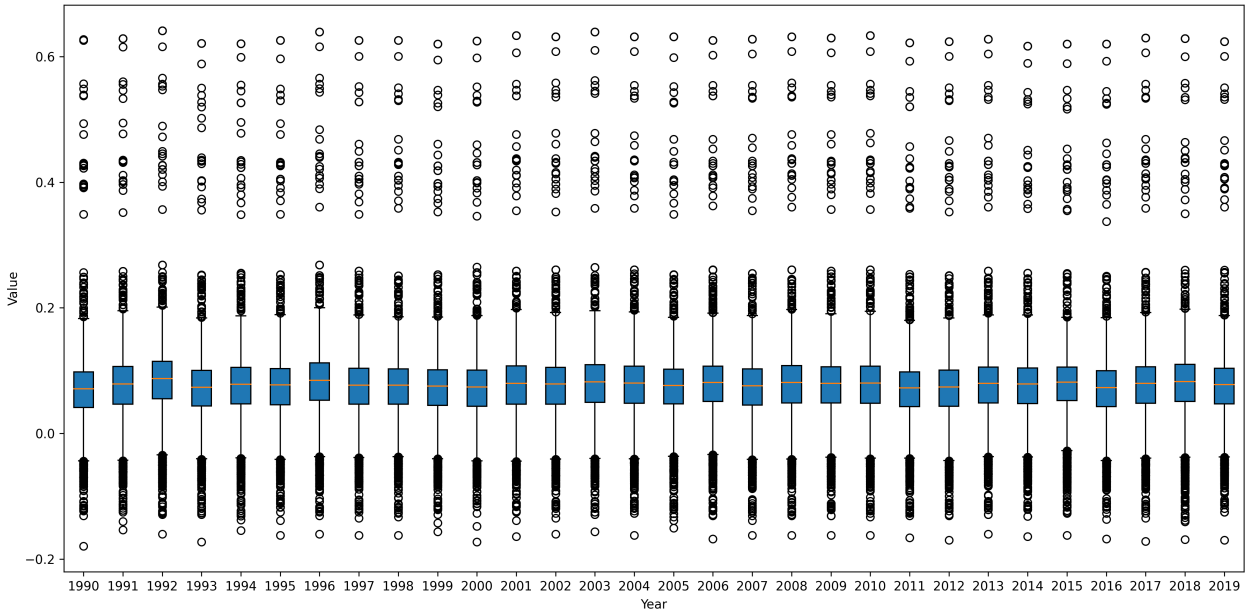
Supplementary Table 2: States of the winter NAO index splitted into quintiles. Quantile values τ depicted in the second row. The third and fourth rows represent the corresponding values of the winter NAO index for the "old" and "new" data.



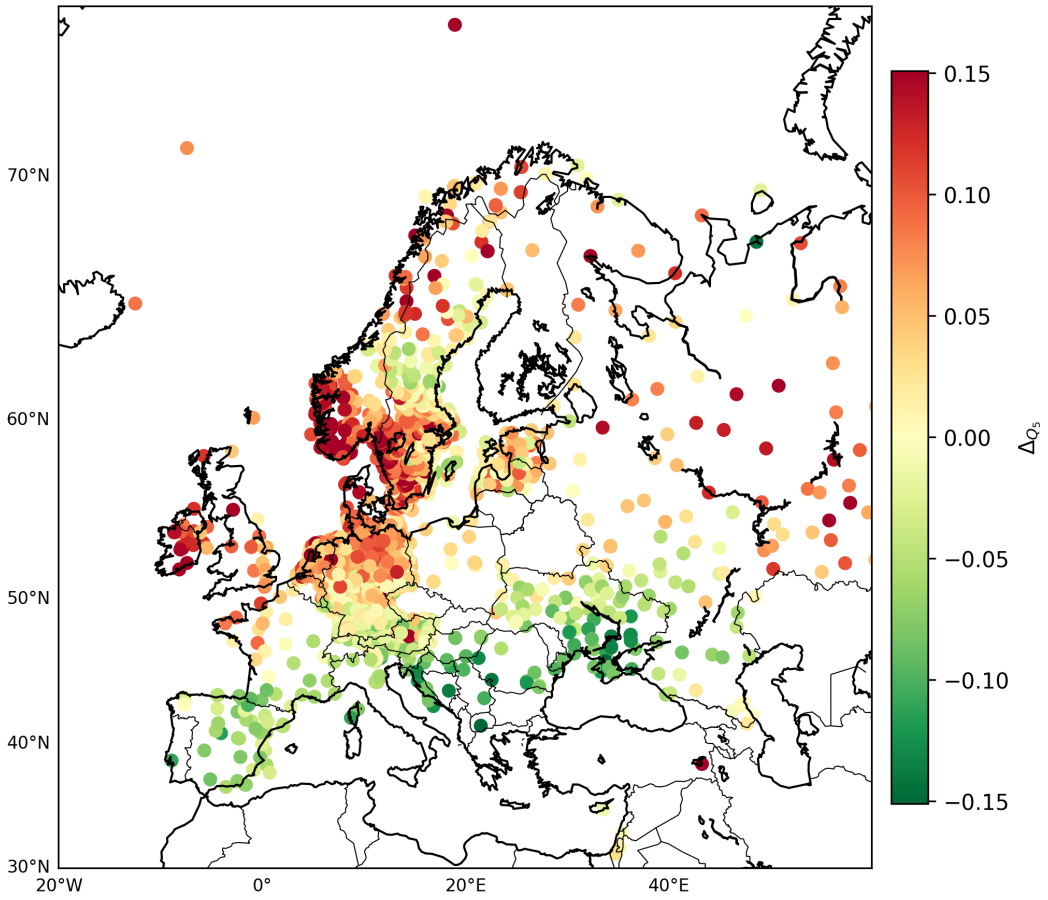
Supplementary Figure 10: Probabilities of rain conditional on the respective quintile of the NAO index with 95% confidence bounds.



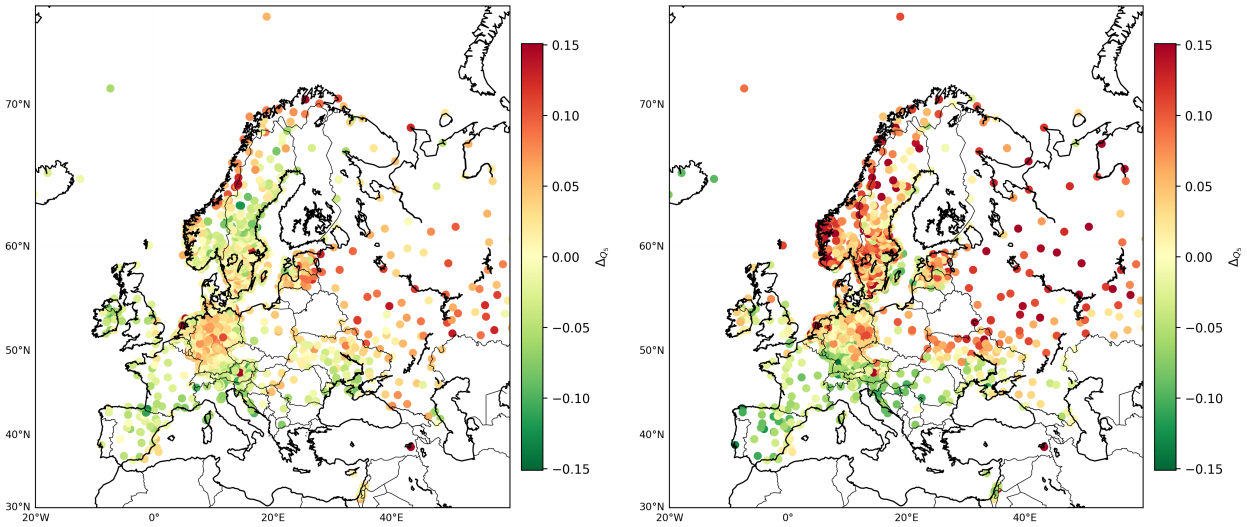
Supplementary Figure 11: Figure 5(a) where stations with insignificant Δ_{i,Q_t} are removed.



Supplementary Figure 12: Boxplots for Δ_{Q_5} for weather stations across Europe when one year is left out. The horizontal axis denotes the year that is excluded from the analysis. The boxplots present the distribution of Δ_{Q_5} when one year is excluded.



Supplementary Figure 13: Δ_{i,Q_1}^{SCAND} for weather stations across Europe.



(a) Δ_{i,Q_1}^{AMO} **(b)** Δ_{i,Q_5}^{AMO}

Supplementary Figure 14: Δ_{i,Q_j}^{AMO} for $j = 1$ in (a) and $j = 5$ in (b) for weather stations across Europe.

Parameter	$\tau = 0.1$		$\tau = 0.5$		$\tau = 0.9$	
	90% CI	95% CI	90% CI	95% CI	90% CI	95% CI
$\alpha_0(\tau)$	89.36%	94.24%	91.96%	96.42%	89.20%	94.52%
$\alpha_1(\tau)$	89.54%	93.92%	90.98%	95.60%	91.60%	95.38%
$\alpha_{1,2}(\tau)$	88.42%	93.72%	92.46%	96.58%	92.56%	96.24%
$\alpha_{1,3}(\tau)$	91.74%	96.30%	90.62%	95.40%	92.44%	96.40%
$\alpha_{2,2}(\tau)$	87.80%	93.50%	91.18%	95.58%	88.20%	93.54%
$\alpha_{2,3}(\tau)$	85.34%	91.54%	89.90%	95.02%	88.08%	93.96%
$\beta_0(\tau)$	85.70%	92.16%	88.98%	94.36%	87.84%	93.30%
$\beta_{1,1}(\tau)$	83.96%	90.74%	91.28%	96.10%	91.04%	95.44%
$\beta_{1,2}(\tau)$	87.66%	92.92%	86.68%	92.26%	87.40%	93.20%
$\beta_{2,1}(\tau)$	86.26%	91.86%	89.14%	94.08%	88.10%	93.38%
$\beta_{2,2}(\tau)$	87.04%	92.50%	89.22%	94.54%	89.90%	94.42%

Supplementary Table 3: Empirical coverage rates of a Monte Carlo study with 5000 Monte Carlo iterations to verify the validity of the asymptotic distribution of the parameters. The vertical axis denotes the parameters and the horizontal axis denotes the quantile levels τ and the nominal levels. Initial parameters are the parameter estimates obtained by fitting model (1) to the data in De Bilt from 1990-2020.